Petroleum Science 18 (2021) 1650–1661

Contents lists available at ScienceDirect

Petroleum Science

journal homepage: www.keaipublishing.com/en/journals/petroleum-science

Original Paper

First-order multiples imaging aided by water bottom

Yan-Bao Zhang [a], Yi-Ke Liu [b, *], Jia Yi [c], Xue-Jian Liu [b, d]

[a] Institute of Geophysics, China Earthquake Administration, Beijing, 100081, China
[b] Key Laboratory of Petroleum Resources Research, Institute of Geology and Geophysics, Chinese Academy of Sciences, Beijing, 100029, China
[c] China Earthquake Disaster Prevention Center, China Earthquake Administration, Beijing, 100029, China
[d] The Pennsylvania State University, Department of Geosciences, University Park, PA, 16802, USA

ARTICLE INFO

Article history:
Received 6 October 2020
Accepted 29 March 2021
Available online 21 September 2021

Edited by Jie Hao and Teng Zhu

Keywords:
Surface-related multiples
Multiples imaging
Multiples elimination

ABSTRACT

Surface-related multiples frequently propagate into the subsurface and contain abundant information on small reflection angles. Compared with the conventional migration of primaries, migration of multiples offers complementary illumination and a higher vertical resolution. However, crosstalk artifacts caused by unrelated multiples during reverse time migration (RTM) using multiples severely degrade the reliability and interpretation of the final migration images. Therefore, we proposed RTM using first-order receiver-side water-bottom-related multiples for eliminating crosstalk artifacts and enhancing vertical resolution. We first backward propagate the first-order receiver-side water-bottom-related multiples using a water-layer model, followed by saving the upper boundary wavefield. Then we produce the source wavefield using a seismic wavelet and the receiver wavefield by back-extrapolating the saved boundary. Finally, the cross-correlation imaging condition is applied to generate the final image. This method transforms the receiver-side multiples into primaries, followed by the conventional migration processing procedures. Numerical examples using synthetic datasets demonstrate that our method significantly enhances the imaging quality by eliminating crosstalk artifacts and improving the resolution.

1. Introduction

Conventional imaging algorithms are usually designed to migrate primaries, with multiples generally recognized as noise that requires suppression in advance (Verschuur et al., 1992; Dragoset et al., 2010; Shi and Wang, 2012; Zhou et al., 2019; Bai et al., 2020). Multiples are reflections that bounce more than once between subsurface interfaces. Although these include surface-related multiples and internal multiples, in this study, we concentrate on the applications of the surface-related multiples. Surface-related multiple elimination (SRME) algorithm is developed and is one of the most commonly used methods for the suppression of surface-related multiples. In this approach, the multiples are predicted by applying a time-domain convolution or a frequency-domain multiplication of the seismic data (Verschuur et al., 1992; Berkhout and Verschuur, 1997). Surface-related multiples can complement illumination in the shadow zones of primaries, as they propagate longer than primaries along different paths. And surface-related multiples are characterized by abundant smaller reflection angles than those of the corresponding primaries, thereby producing images with higher vertical resolutions. Recently, imaging through multiples has been widely explored (Muijs et al., 2007; Zuberi and Alkhalifah, 2013; Lu et al., 2015; Li et al., 2017; Davydenko and Verschuur, 2017; Liu and Liu, 2018a), however, many challenges are still encountered in this endeavor.

Based on the two-way wave equation, reverse time migration (RTM) can provide high-quality seismic imaging results of complex geological structures (Baysal et al., 1983). To exploit multiples in RTM, Liu et al. (2011) proposed RTM using multiples (RTMM) to reconstruct subsalt structures. Compared to the conventional RTM, in the RTMM, the source signature is replaced by the recorded data (containing primaries and multiples) and the multiples (isolated by SRME) are regarded as the receiver wavefield before the imaging condition is implemented. Additionally, Zuberi and Alkhalifah (2013) proposed the simultaneous backward and forward extrapolation of the raw data (including direct wave). Imaging methods utilizing multiples exhibit many advantages such as additional

* Corresponding author.
E-mail address: ykliu@mail.iggcas.ac.cn (Y.-K. Liu).

https://doi.org/10.1016/j.petsci.2021.09.036

illumination and a higher vertical resolution. However, RTMM suffers from severe artifacts of undesired interferences of unrelated multiples. The crosstalks degrade the imaging quality and drastically contaminate the true migration images. Lu et al. (2015) classified crosstalks into causal and anticausal components, whereas, Zhang et al. (2020) classified these into order-related and event-related components. Multiples can be sorted into different order components, and the order of multiples is defined by the number of bounces at the free surface. The order-related crosstalk components are produced by interactions between different-order multiples, while event-related crosstalk components occur when two or more events illuminate the same reflector. Both crosstalk categories result in severe damage to the final imaging results derived from multiples.

Through minimizing the objective function between the predicted and observed data, the least-squares reverse time migration (LSRTM) provides images of complex geological structures involving balanced amplitudes and high resolutions (Nemeth et al., 1999; Luo and Hale, 2014; Yao and Wu, 2015; Liu et al., 2017; Rocha and Sava, 2018; He et al., 2019). LSRTM can be extended to multiples migration and crosstalk suppression partially by minimizing the misfit function between the predicted multiples (generated by the Born modeling) and the observed multiples (separated by the SRME) (Zhang and Schuster, 2014; Liu et al. 2016, 2018, 2018b, 2018; Liu et al., 2018b). However, LSRTM is expensive and affected by many practical issues including producing multisolutions and poor-convergence problems. Therefore, LSRTM using multiples cannot guarantee to supply good multiple imaging results.

In marine streamer datasets, multiples related to the water layer are energetic because the air/water and water/sediments interfaces have high impedance contrasts. A source-side (receiver-side) water-bottom-related multiple is defined as a free-surface multiple involving several bounces between the free surface and the water bottom on the source (receiver) side and one round of travel between the free surface and the subsurface reflectors on the receiver (source) side. The source-side water-bottom-related multiples contribute to expanding the illumination, while the receiver-side multiples can provide more abundant information on the small reflection angles than the corresponding primaries. These smaller reflection angles permit a higher vertical resolution. Zhang et al. (2020) conducted migration using the source-side water-bottom-related multiples to generate imaging results without crosstalks and with additional illumination. Similarly, the receiver-side water-bottom-related multiples can also be adequately migrated to provide suitable information regarding subsurface structures. Fig. 1 illustrates the raypaths of two first-order water-bottom-related multiples, with Sa'b'c'R and SabcR representing the source-side and receiver-side components, respectively. These multiples can be obtained through frequency-domain multiplication or a time-domain convolution between the primaries isolated by SRME and the water-column primaries produced by wave-equation modeling using a water layer model. The water-column primary represents a primary that only propagates in the water layer without ever going below the water bottom. Therefore, to exploit the information of smaller reflection angles of receiver-side multiples, we developed RTM using the first-order receiver-side water-bottom-related multiples (RTM-FRWM) to form crosstalk-free and high-resolution images. This method transforms the receiver-side multiples into virtual primaries by extrapolating backward before applying the conventional migration approaches. The proposed imaging algorithm employs the same cross-correlation imaging condition as that of traditional RTM for primaries. Through numerical experiments, this method was shown to be a potential imaging complement to that from primaries in complex geologic settings by numerical experiments.

This paper is organized as follows: First, we introduce the RTMM and analyze the crosstalk artifacts generation briefly. Then, the proposed RTM-FRWM is described in detail, and the isolation algorithm of multiples utilized is specified. Synthetic examples of one simple and two complex models are then used to validate the feasibility and effectiveness of the developed approach, followed by the discussions and conclusions in the final section.

2. Methodology

2.1. RTMM and crosstalk artifacts analysis

Liu et al. (2011) propose RTMM to utilize multiple reflections in imaging subsalt structures. Compared to the conventional RTM, RTMM replaces the source wavelet with the recorded data, taking the estimated multiples as the receiver data instead of primaries. The zero-lag cross-correlation imaging condition is then implemented to produce the subsurface structure image I_M expressed as follows:

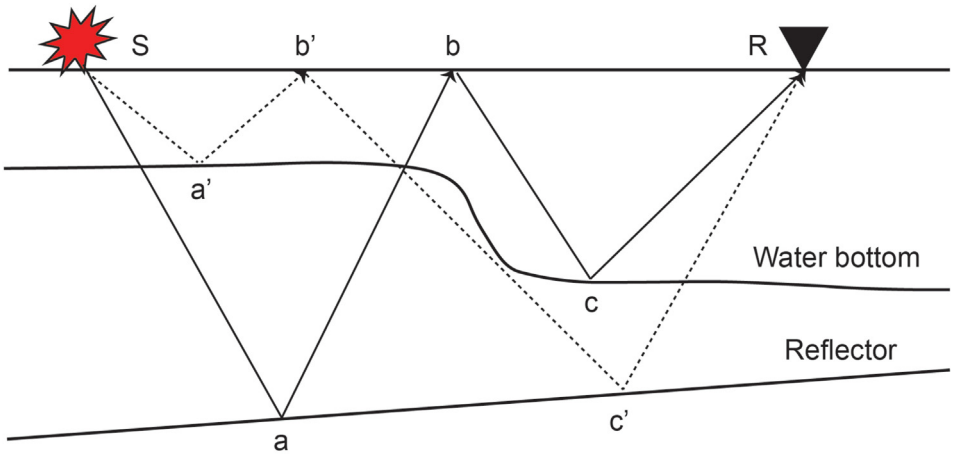

Fig. 1. Raypath diagrams of first-order water-bottom-related multiples. The dotted raypath Sa'b'c'R and solid raypath SabcR illustrate the source-side and receiver-side first-order water-bottom-related multiples, respectively. The multiples of interest in this research contain the first-order water-column multiples and receiver-side peg-leg multiples.

$$I_M = \sum_{t=0}^{t_{\max}} F(x,z,t)B(x,z,t) \tag{1}$$

where F denotes the forward propagating source wavefield, B indicates the backward propagating receiver wavefield, and $t_{\max}$ is the maximum recording time. The forward- and backward-propagating multiples can be divided into pairs of related and unrelated multiples. The related multiples are defined as a pair of multiples in which the $(n+1)$th-order multiples (backward propagating) are generated by the nth-order multiples (forward propagating). If the forward-propagating jth-order and the backward-propagating ith-order multiples are satisfied with the condition $j \neq i-1$, the pair of multiples is defined as unrelated multiples. In RTMM, only crosscorrelations between the related multiples pairs contribute to correcting the imaging points while interactions among the unrelated multiples produce crosstalk artifacts. Therefore, multiple imaging results can be expressed as follows:

$$I_M(x,z) = I_R(x,z) + I_U(x,z) \tag{2}$$

where $I_R(x,z)$ represents the correct image produced by the related multiples pairs, and $I_U(x,z)$ denotes the crosstalks generated by unrelated multiples. By selecting pairs of related multiples to perform a migration, for example, the water-column primaries and first-order source-side water-bottom-related multiples pair, result without crosstalks can be obtained. If the source wavelet is considered as negative first-order multiples and the primaries as zeroth-order multiples, the source wavelet and primaries pair represents a special case of related multiples.

2.2. RTM using first-order receiver-side water-bottom-related multiples (RTM-FRWM)

The free surface and interfaces with strong impedance contrast such as the seafloor and the top and bottom of salt structures generate strong surface-related multiples in seismic data recorded using marine acquisition geometry. Compared with other strong multiples, the water-bottom-related multiples are easily obtained through a water-layer model. Therefore, RTM-FRWM was developed by exploiting the small reflection angles of multiples and to eliminate crosstalk artifacts. The first-order receiver-side water-bottom-related multiples can be predicted by convolving primaries with the water-column primaries in the time domain, and detailed steps for producing the specific multiples are provided in the next section. In this method, the first-order receiver-side water-bottom-related multiples are transformed into primaries, followed by the conventional migration processing procedures.

Considering that the sources and receivers are on the free surface, x_s and x_r represent their horizontal positions. In our method, the extracted first-order receiver-side water-bottom-related multiples $m^1_{rw}(x_r,x_s,t)$ are backward extrapolated twice. In the first, we produce the backward-propagated wavefield W^1_B by wave equation backward modeling with the water-layer velocity $v_{wl}(x,z)$ as follows:

$$\begin{cases} \dfrac{1}{v_{wl}(x,z)^2}\dfrac{\partial^2 W^1_B(x,z,t)}{\partial t^2} = \left(\dfrac{\partial^2}{\partial x^2}+\dfrac{\partial^2}{\partial z^2}\right)W^1_B(x,z,t) \\ W^1_B(x_r,z=0,t) = m^1_{rw}(x_r,x_s,t) \end{cases} \tag{3}$$

And then we save the initial boundary data at each backward time step:

$$p_{b1}(x_g,x_s,t) = W^1_B(x_g,z=0,t) \tag{4}$$

where x_g represents the horizontal positions of the upper boundary grid point. The water velocity $v_w(x,z)$ is then used to produce the backward-propagated wavefield W^2_B as:

$$\begin{cases} \dfrac{1}{v_w(x,z)^2}\dfrac{\partial^2 W^2_B(x,z,t)}{\partial t^2} = \left(\dfrac{\partial^2}{\partial x^2}+\dfrac{\partial^2}{\partial z^2}\right)W^2_B(x,z,t) \\ W^2_B(x_r,z=0,t) = m^1_{rw}(x_r,x_s,t) \end{cases} \tag{5}$$

followed by saving the second boundary data at each time step:

$$p_{b2}(x_g,x_s,t) = W^2_B(x_g,z=0,t) \tag{6}$$

The reproduced primaries can be obtained from the following expression:

$$p_r(x_g,x_s,t) = p_{b1}(x_g,x_s,t) - p_{b2}(x_g,x_s,t) \tag{7}$$

The second boundary data $p_{b2}(x_g,x_s,t)$ act as the "direct" wave in the first boundary data $p_{b1}(x_g,x_s,t)$, and this requires subtraction in the pre-processing procedures. Then, the source wavelet $f(t)$ is penetrated into the earth to generate the forward-propagating source wavefield $W_F(x,z,t)$ (Eq. (8)) and the reproduced primaries $p_r(x_g,x_s,t)$ are extrapolated at the upper boundary grids to obtain the backward-propagating receiver wavefield $W_B(x,z,t)$(see Eq. (9)) as follows:

$$\begin{cases} \dfrac{1}{v(x,z)^2}\dfrac{\partial^2 W_F(x,z,t)}{\partial t^2} = \left(\dfrac{\partial^2}{\partial x^2}+\dfrac{\partial^2}{\partial z^2}\right)W_F(x,z,t) \\ W_F(x_s,z=0,t) = f(t) \end{cases} \tag{8}$$

$$\begin{cases} \dfrac{1}{v(x,z)^2}\dfrac{\partial^2 W_B(x,z,t)}{\partial t^2} = \left(\dfrac{\partial^2}{\partial x^2}+\dfrac{\partial^2}{\partial z^2}\right)W_B(x,z,t) \\ W_B(x_g,z=0,t) = p_r(x_g,x_s,t) \end{cases} \tag{9}$$

where $v(x,z)$ represents the migration velocity model. Finally, the zero-lag cross-correlation imaging condition between the source and receiver wavefields is employed to obtain the image of multiples $I(x,z)$, expressed as follows:

$$I(x,z) = \sum_{t=0}^{t_{\max}} W_F(x,z,t)W_B(x,z,t) \tag{10}$$

As illustrated in Fig. 2, the first-order receiver-side water-bottom-related multiples can be migrated to the correct imaging point X1 through the following process: 1) backward-extrapolating the receive-side multiples using a water-layer model as described by the blue raypaths, 2) saving the upper boundary reflection data at R', 3) simultaneously forward-propagating the source wavelet at S and backward-propagating the saved boundary condition as indicated by the red raypaths, and 4) crosscorrelating of the forward and backward propagated waves indicated by the red raypaths. By transforming the first-order receiver-side water-bottom-related multiples into virtual primaries, we can acquire more wave information from small reflection angles, which ultimately promotes higher vertical resolution. Overall, the proposed RTM using the receiver-side multiples provides higher-quality results due to the absence of crosstalks compared with RTMM and yields a higher vertical resolution than the conventional RTM of primaries owing to smaller reflection angles of the receiver-side multiples.

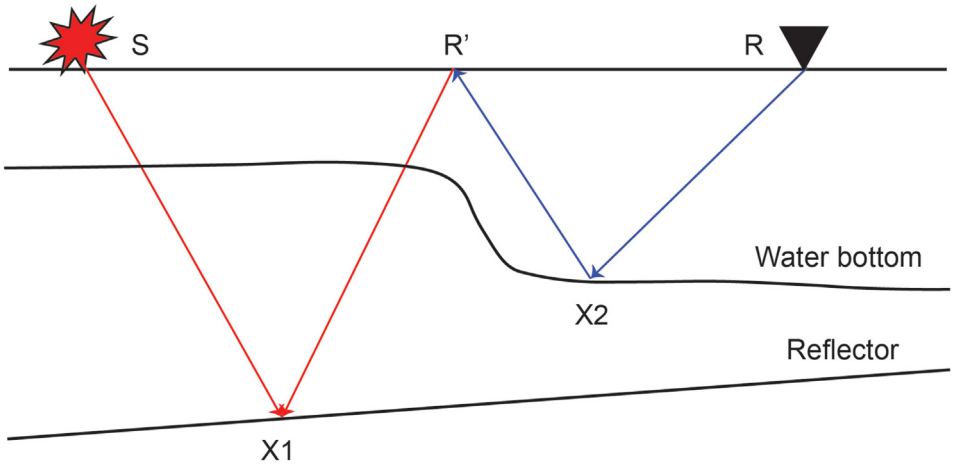

Fig. 2. Illustration of the developed migration method. The image of this proposed method can be acquired by the following two steps: 1) transforming receiver-side multiples into virtual primaries as denoted by the blue raypaths; 2) crosscorrelating the forward- and backward-propagating wave at the imaging point X1 as described by the red raypaths.

2.3. First-order receiver-side water-bottom-related multiples extraction

Provided that the first-order receiver-side water-bottom-related multiples are available, crosstalk artifacts can be avoided, and a higher vertical resolution can be obtained using the developed method. SRME (see Appendix) produces surface-related multiples from the recorded data by stacking convolutions between the common receiver and common source traces. To extract the first-order receiver-side water-bottom-related multiples, we simplified SRME and expressed the separation of the specific multiples as described in the following text.

According to the matrix notation from Berkhout (1982), the recorded primaries can be expressed in the frequency domain as follows:

$$\boldsymbol{P_0} = \boldsymbol{SG} \tag{11}$$

where $\boldsymbol{P_0}$ represents the primaries matrix, $\boldsymbol{S}$ is the source function matrix, and $\boldsymbol{G}$ denotes the Green's function to the response of subsurface structures. The primaries $\boldsymbol{P_0}$ are separated from the regular SRME as exhibited in Appendix A. The full first-order water-bottom-related multiples can be acquired from the convolutions between the primaries and the Green's function's response to the water-bottom $\boldsymbol{G_w}$ through the following expressions:

$$\begin{cases} \boldsymbol{M^1_{ws}} = \boldsymbol{G_w P_0} \\ \boldsymbol{M^1_{wr}} = \boldsymbol{P_0 G_w} \end{cases} \tag{12}$$

where $\boldsymbol{M^1_{ws}}$ and $\boldsymbol{M^1_{wr}}$represent the first-order source-side and receiver-side water-bottom-related multiples, respectively. The Green's function $\boldsymbol{G_w}$ can be obtained by wave-equation modeling using a known water-bottom velocity model (Wang et al., 2011; Jin and Wang, 2012; Yao et al., 2018) or by statistical estimation from the primaries statistically (Biersteker, 2001; Hargreaves, 2006). After implementing the lower part of Eq. (12), we adaptively matched the predicted first-order receiver-side water-bottom-related multiples with the original data to extract the actual first-order receiver-side water-bottom-related multiples.

2.4. Workflow

The workflow for migrating the first-order receiver-side water-bottom-related multiples is summarized in the following steps:

1) Produce the water-column primaries with the water-layer model through wave-equation modeling, and then, adaptively match these with the recorded data to obtain real water-column primaries.
2) Separate the primaries from the recorded data using SRME in Eq. (13).
3) Convolve the estimated primaries with the water-column primaries to get the predicted first-order receiver-side water-bottom-related multiples using Eq. (12) and subsequently, match these with the recorded data to adaptively generate the estimated receiver-side multiples.
4) Backward penetrate the first-order receiver-side water-bottom-related multiple using a water-layer model and the water velocity, and then produce the upper boundary data using Eqs. (3) and (5), respectively. The reproduced primaries are the differences between the two sets of boundary data (Eq. (7)).

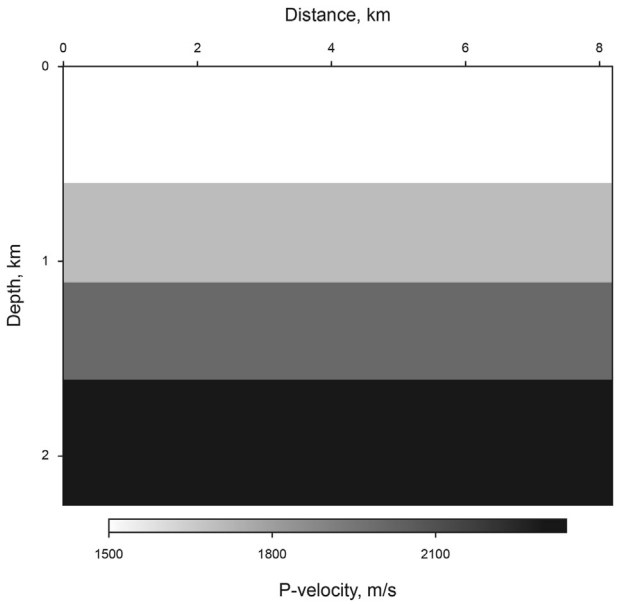

Fig. 3. The four-layer velocity model.

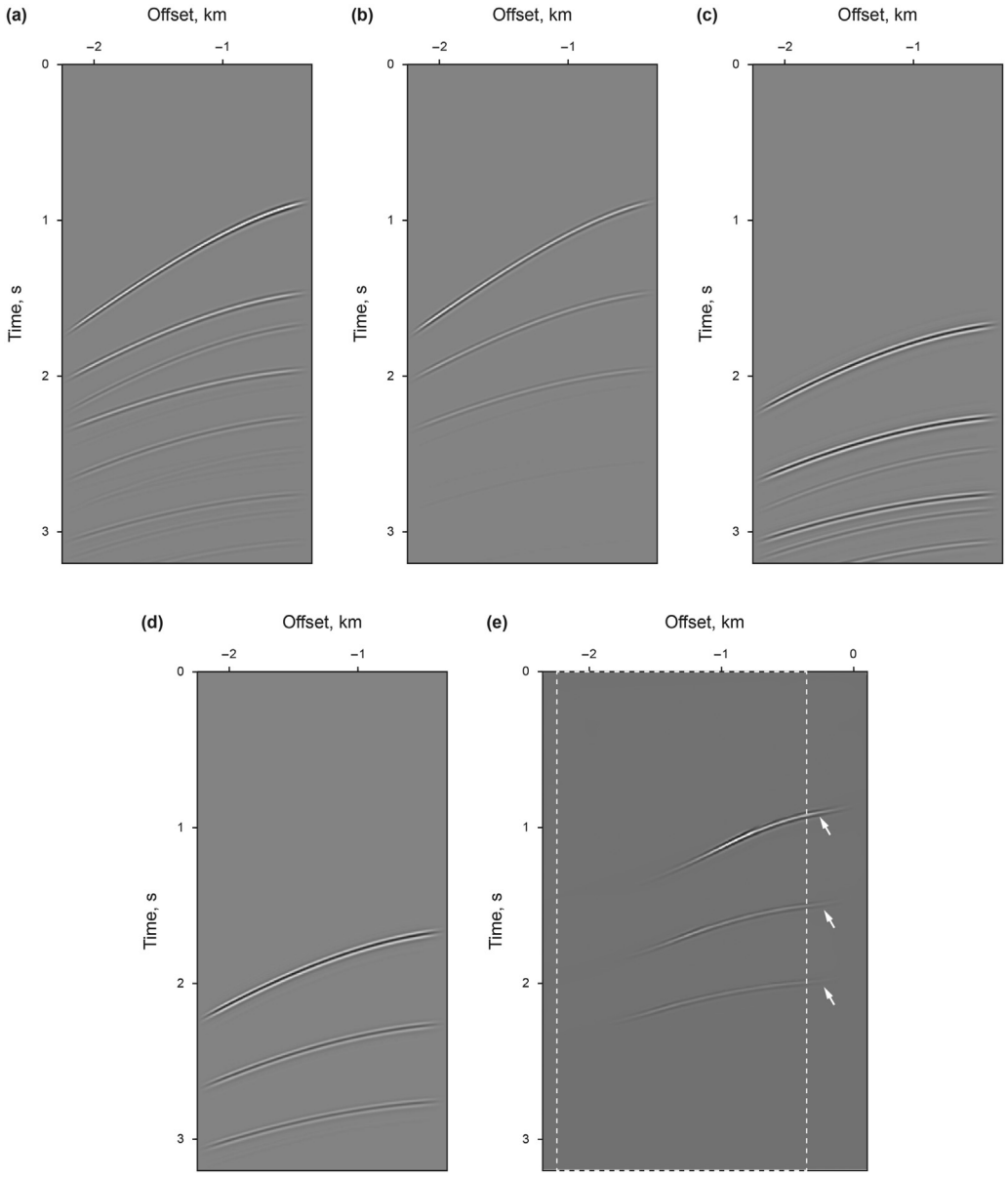

Fig. 4. Separation results of different-order multiples for the four-layer model. (a) One original shot gather, (b) primaries isolated by SRME, (c) all-order multiples separated using SRME, (d) first-order receiver-side water-bottom-related multiples, and (e) the reconstructed virtual primaries. The dashed rectangle in panel e represents the correct location of original recording length, and the white arrows indicate that we can produce more useful information of near offset (small angle).

5) Create the subsurface image through crosscorrelation (Eq. (10)) between the source wavefield generated by injecting the seismic wavelet (Eq. (8)) and the receiver wavefield obtained by regarding the reproduced primaries as the backward propagating data (Eq. (9)).

3. Numerical experiments

3.1. A four-layer velocity model

The first synthetic experiment is on a simple layer velocity model with three flat interfaces, as displayed in Fig. 3. This model composes of 1650 grid points along the horizontal direction and 451 grid points along the vertical direction both with an interval of 5 m. A set of 193 shot gathers distributed from 2.25 to 8.01 km with a 30-m shot interval is used to test the performances of different methods. The source and receiver depths are both 5 m. The source signature is a Ricker wavelet with a dominant frequency of 20 Hz. Each shot gather has 388 receivers with a 5-m receiver interval and 401 time samples with an 8-ms sampling interval. And the maximum and minimum negative offsets of shot gathers are −2.245 km and −0.31 km, respectively. Before implementing different migration methods, we need to supply the forward- and backward-propagating data. Fig. 4 displays the separated results of different-order multiples. The primaries in Fig. 4b and all-order multiples in Fig. 4c are separated from the original shot gather (Fig. 4a) using SRME. The first-order receiver-side water-bottom-related multiples are predicted by convolving the estimated primaries with the water-column primaries, ordered by severity. We then adaptively match the predicted multiples with the original shot gather to extract the actual first-order receiver-side water-bottom-related multiples, as shown in Fig. 4d. Fig. 4e shows the

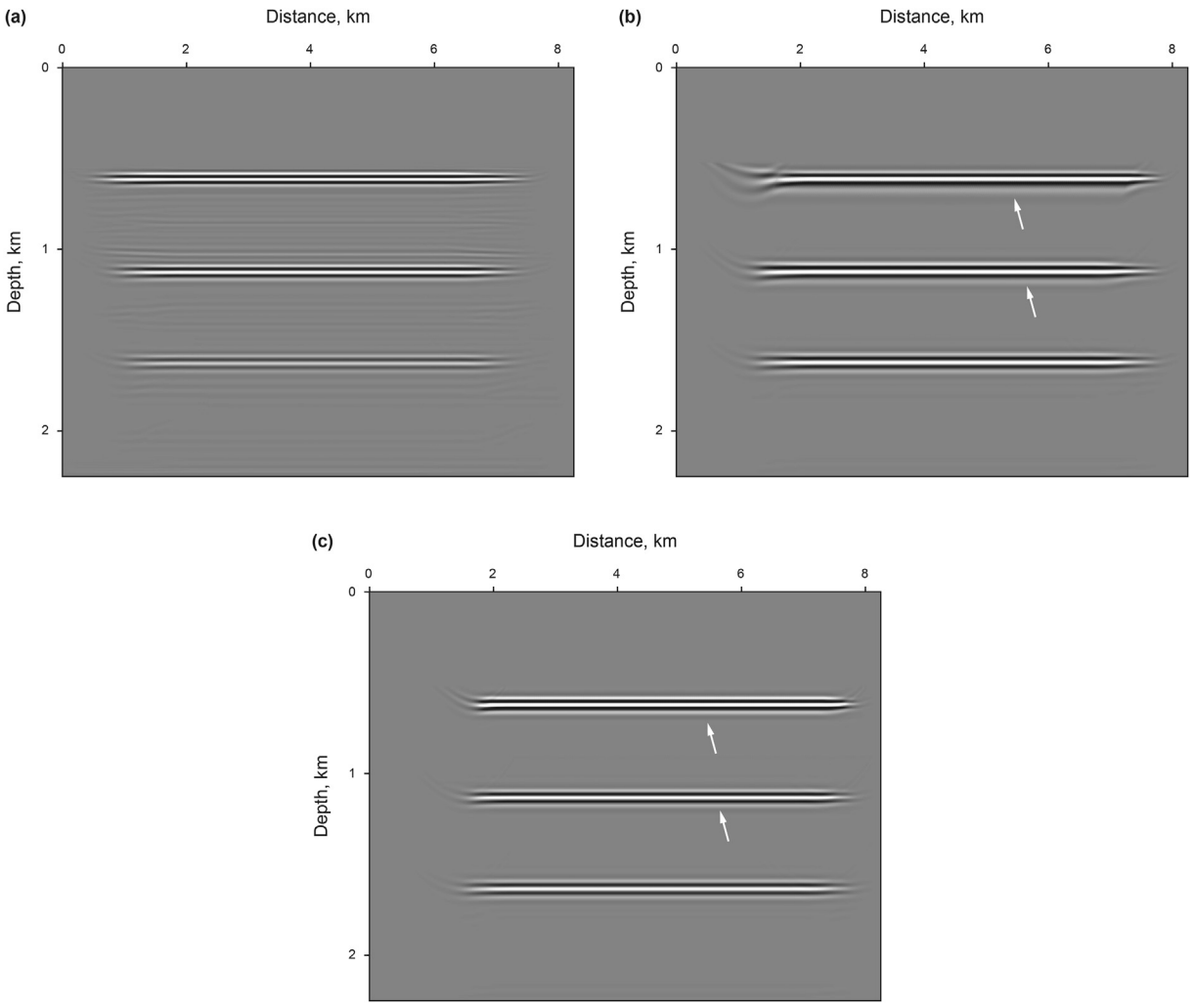

Fig. 5. Migration results for the four-layer model. (a) RTM of all-order multiples (RTMM), (b) RTM of primaries only, (c) RTM of the first-order receiver-side water-bottom-related multiples (RTM-FRWM). The white arrows indicate that RTM-FRWM (panel c) can generate a result with a higher vertical resolution by exploiting the small angle information of multiples when compared with conventional RTM (panel b).

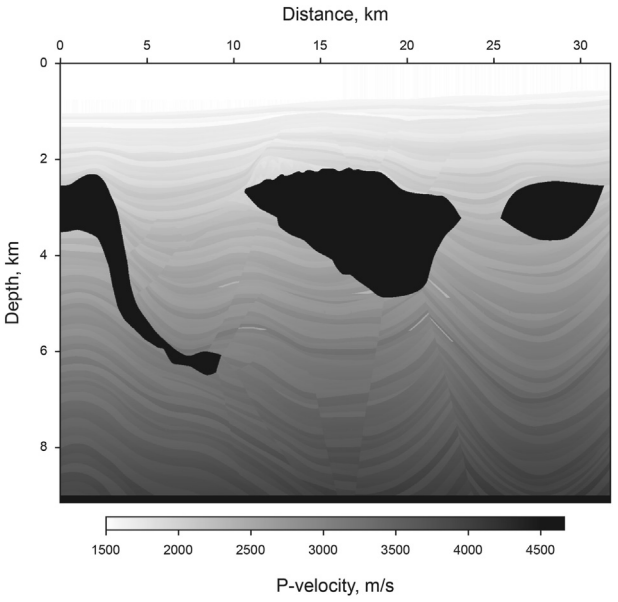

Fig. 6. The Pluto 1.5 P-wave velocity model.

reconstructed virtual primaries by backward-propagating the data in Fig. 4d, and as indicated by the white arrows, we can produce more useful information of near offset (small angle). Applying different migration algorithms to different forward- and corresponding backward-propagating data can produce different images, as displayed in Fig. 5. Fig. 5a shows the imaging results of all-order multiples, in which we can observe there are 3 strong events and several visual crosstalk events between different interfaces resulting from interferences among unrelated multiples. As we expected conventional RTM using primaries can generate a clear image in Fig. 5b and no visible artifacts can be seen. To eliminate crosstalks and make the most of small angle information of multiples, we applied RTM-FRWM to the data in Fig. 4d. The image (Fig. 5c) is generated following the workflow in the previous section. Compared with RTMM, RTM-FRWM can remove almost all crosstalk artifacts and yield results with higher S/N ratios. As the white arrows indicate in Fig. 5b and c, RTM-FRWM can generate a result with a higher vertical resolution by exploiting the small angl information of multiples when compared with conventional RTM. The experiments on the four-layer velocity model demonstrate that the new approach can produce clear and high-resolution results.

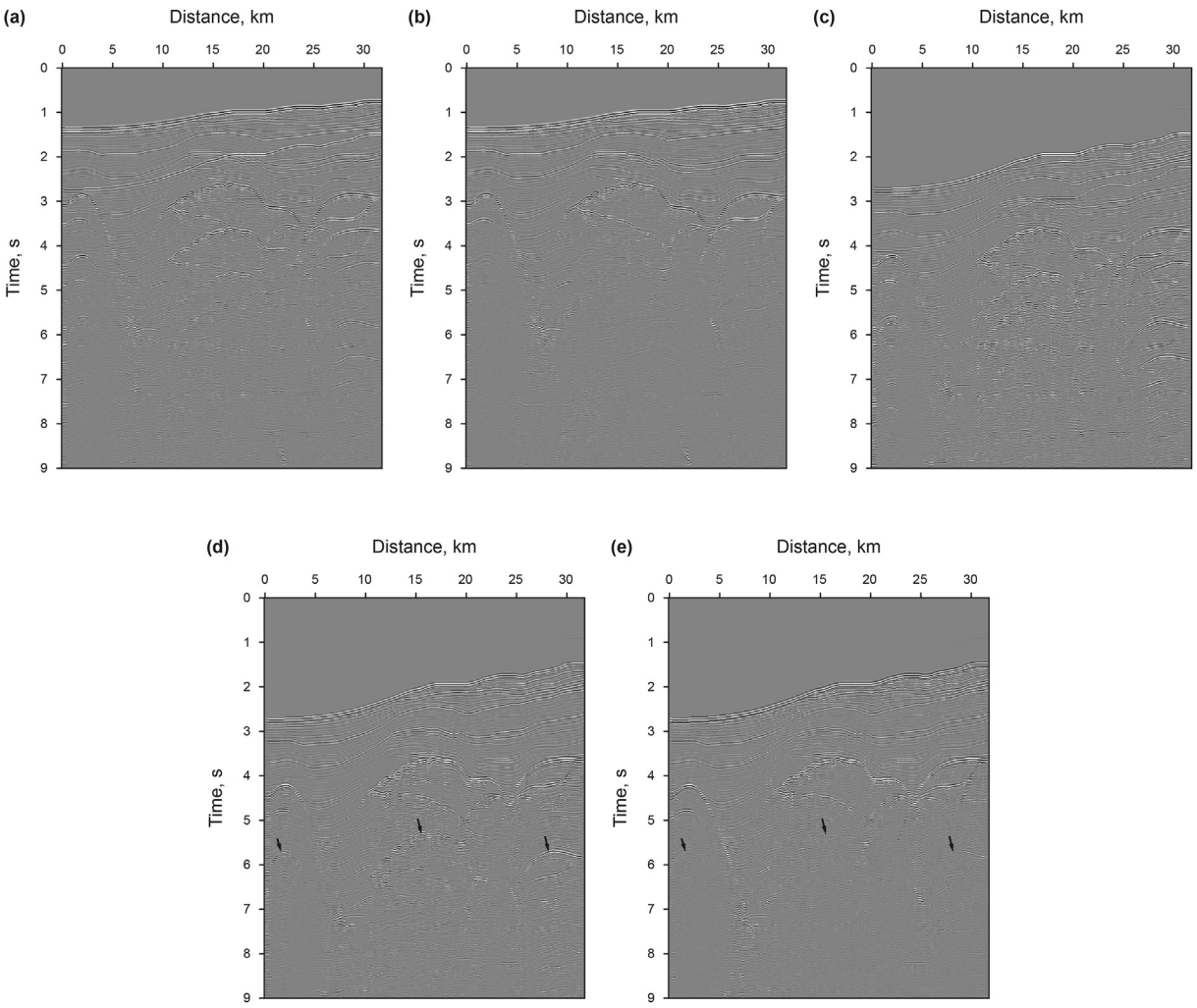

Fig. 7. The near-offset stack profiles of (a) the original data, (b) the primaries, (c) multiples, (d) the first-order multiples, (e) The first-order receiver-side water-bottom-related multiples. The black arrows in panel (e) indicate that the redundant illuminating events have been well suppressed in the first-order receiver-side water-bottom-related multiples.

3.2. The Pluto 1.5 model

The Pluto 1.5 velocity model comprising of 1201 vertical grid points with a 7.62 m interval and 1387 horizontal grid points with a 22.86 m interval is displayed in Fig. 6. These data retrieved from the SMAART JV consortium involved 232 sources with a source interval of 137.16 m on the top surface of the model. The source time function is a Ricker wavelet with a dominant frequency of 15 Hz. We transformed the shot gather from the split-spread data into the towed-streamer data by decimating the original 540 traces into 173 traces with a −160.02 m minimum near offset. The total recording time is 9 s, and the sampling time is 8 ms.

Fig. 7 shows the near-offset stack profiles of different types of data. The original data comprising of primaries and multiples are displayed in Fig. 7a. The primaries (Fig. 7b) and multiples (Fig. 7c) can be separated using SRME. The first-order multiples which are extracted using Eq. (15) are exhibited in Fig. 7d. The first-order receiver-side water-bottom-related multiples can be predicted through the convolution between the primaries and the water-column primaries using the lower part of Eq. (12). We then adaptively matched the predicted multiples with the original shot gathers to extract the real first-order water-bottom-related multiples, as shown in Fig. 7e. Compared with the first-order multiples, the stack profile of first-order receiver-side water-bottom-related multiples shows a higher signal-to-noise ratio (S/N). Many events illuminate the same three salt structures as indicated by the black arrows in the first-order multiples near-offset stack profile (Fig. 7d). Notably, the stack profile of the first-order receiver-side water-bottom-related multiples exhibits similarities to that of the primaries, excluding the travel time. Furthermore, upon appreciate backward-extrapolation of the first-order receiver-side multiples, the traveltime differences can be eliminated, thereby producing high-quality imaging results using the proposed method.

Fig. 8 illustrates the RTM images using all orders of multiples (Fig. 8a), the first-order multiples (Fig. 8b), the primaries (Fig. 8c), and the first-order receiver-side water-bottom-related multiples (Fig. 8d). Note that artifacts in the water layer in all images have been muted. Compared with the conventional RTM image of primaries, crosstalk artifacts in the RTM image using all order multiples due to interactions among unrelated forward- and backward-propagating multiples are visible as indicated by black arrows. These artifacts blur the real structures and reduce the S/N of the migration image, subsequently leading to incorrect geological interpretation. In a traditional processing sequence, multiples are considered as noise and suppressed from the primaries. However, multiples also contain useful signals that provide significant information about subsurface structures, such as their smaller reflection angles, as compared to the corresponding primaries.

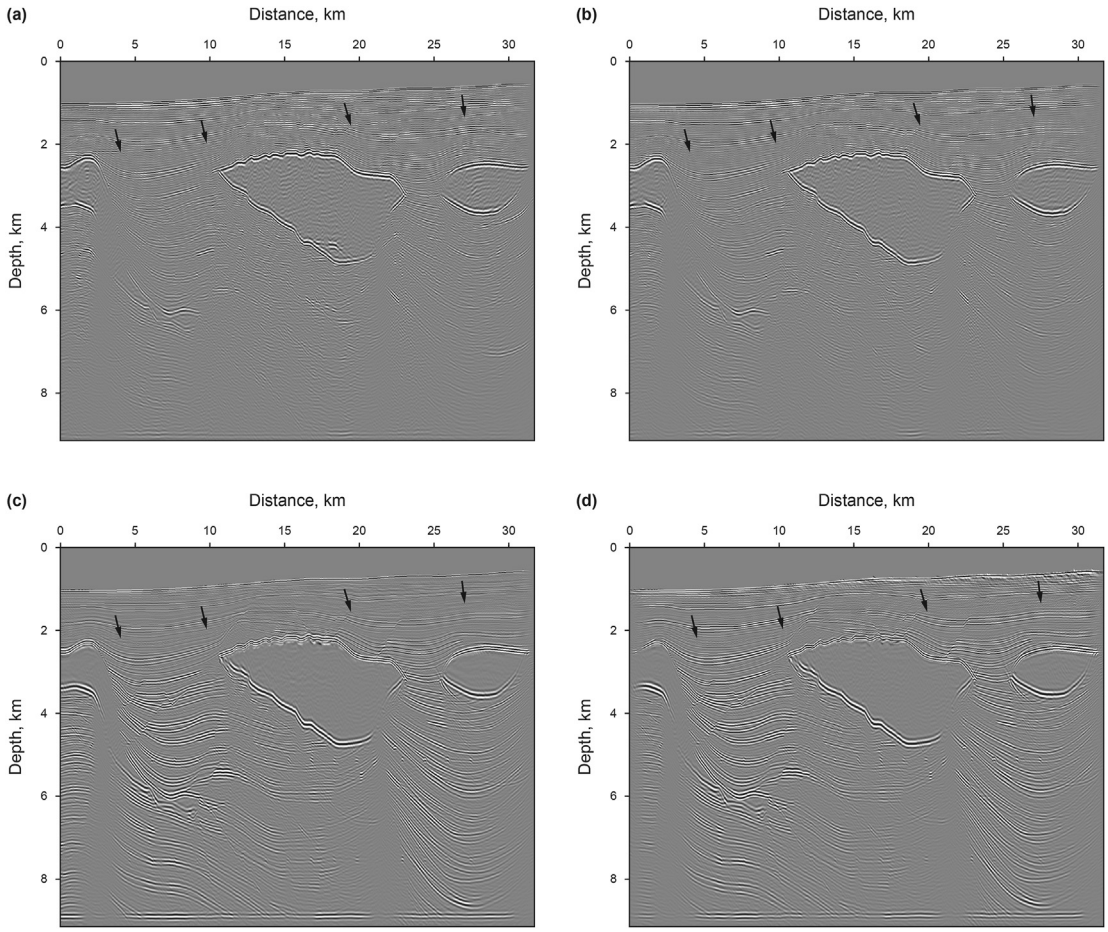

Fig. 8. Migration results of the Pluto 1.5 model. (a) RTM using all orders of multiples, (b) RTM using the first-order multiples, (c) Traditional RTM using primaries, and (d) RTM result by the proposed method.

Consequently, to avoid crosstalk artifacts and utilize the smaller angle information, the first-order multiples and the first-order receiver-side water-bottom-related multiples were migrated. Compared with the image of all-order multiples, the image of first-order multiples in Fig. 8b can eliminate some evident crosstalks, such as the crosstalk which is parallel with the sea bottom indicated by the black arrows. However, RTM using first-order multiples generates results with a low S/N ratio due to the residual of crosstalks (Zhang et al., 2019). To further enhance the imaging quality and reduce crosstalks, we implemented the proposed method. The image of first-order receiver-side water-bottom-related multiples in Fig. 8d is of improved quality and without crosstalk artifacts. The deep structures reconstructed in Fig. 8d are of better quality than those in Fig. 8a and b. The sufficient smaller reflection angles of the first-order receiver-side water-bottom-related multiples make it possible to supply a higher vertical resolution compared with the image of primaries. Magnified views of RTM using all-order multiples, the first-order multiples, the primaries, and the first-order receiver-side water-bottom-related multiples in Fig. 8a-d are displayed in Fig. 9a to d, respectively. As the black arrows indicate, RTM using the first-order multiples can remove energetic crosstalks due to the simplifications of forward- and backward-propagating data. Compared with RTMM and RTM using the first-order multiples, as we expected conventional RTM and RTM-FRWM can produce migration results without crosstalks, however, both the latter two approaches cannot delineate the bottom boundaries of the salt accurately, as shown by the white arrows. The magnified view of the RTM-FRWM image (Fig. 9d) reveals enhanced results of the observed strata above the salt compared with RTM using the first-order multiples (Fig. 9b). Compared with conventional RTM of primaries (Fig. 9c), RTM-FRWM produced an image with a higher vertical resolution and delineated the upper salt boundaries better, as indicated by the red arrows.

3.3. The Sigsbee2B model

To further validate the feasibility and effectiveness of the proposed approach, we applied it to the Sigsbee2B velocity model illustrated in Fig. 10. The model was discretized into 601 $\times$ 1001 grids with a 10 m gridpoint separation. A set of 153 shot gathers evenly distributed from 3.92 to 10.00 km with a 40 m source interval was employed for the imaging. The peak frequency of the Ricker wavelet used was 15 Hz. Each shot gathers involved 250 receivers at 10 m intervals for a depth of 10 m and 1500 time samples linked to an 8 ms sampling interval, with maximum and minimum negative offsets of -3 and -0.51 km, respectively.

Fig. 11 shows different kinds of seismic data. The primaries and the multiples are separated using standard SRME as shown in Fig. 11a and b, respectively. The first-order receiver-side water-bottom-related multiples (see Fig. 11c) can be well extracted by implementing a time-domain convolution (or a frequency-domain multiplication) between the primaries and the water-column primaries using Eq. (12).

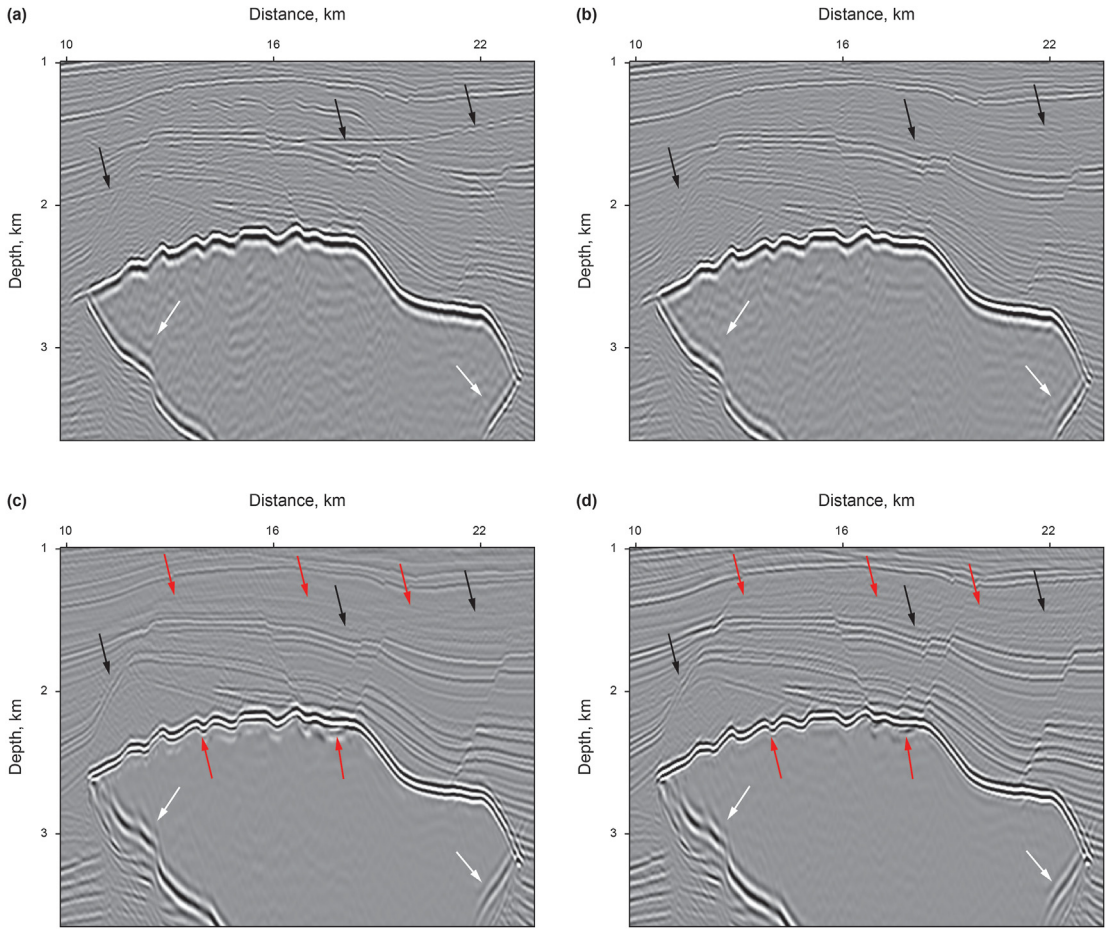

Fig. 9. Panels (a)–(d) are the close-up views of Fig. 8a to d, respectively. The strata are better delineated by the proposed method as pointed out by the red arrows.

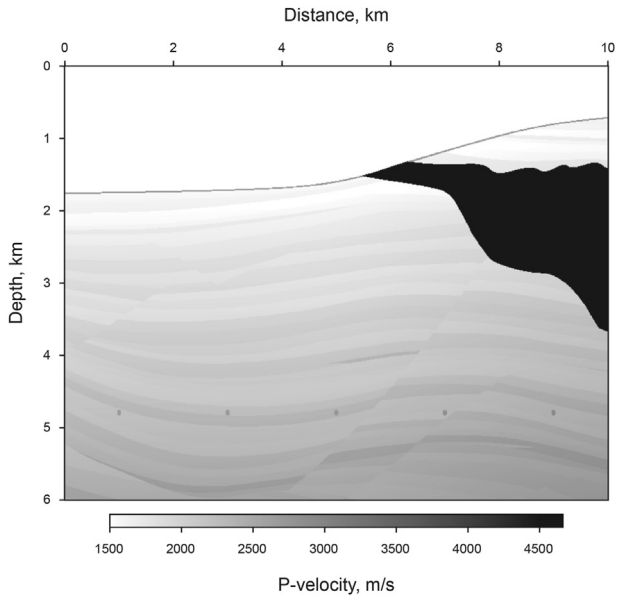

Fig. 10. The partial Sigsbee2B velocity model.

The imaging results obtained from different approaches are shown in Fig. 12. The image from the free-surface multiples in Fig. 12a is severely degraded by the crosstalk artifacts covering subsurface structures compared with that from the primaries in Fig. 12b. The image after applying our method to eliminate the crosstalk artifacts is displayed in Fig. 12c. Taking the primaries image as a reference, the multiples image exhibits a lower S/N ratio and the image of the new method can avoid some false images and reveal the correct strata. As indicated by the black ellipse in Fig. 12a, these structures cannot be revealed by the conventional migration of multiples due to crosstalk artifacts. Compared with the primaries image, the image from our method evidently involves a higher vertical resolution, as displayed by the ellipses in Fig. 12b and c.

4. Discussions

Although the RTM-FRWM can provide subsurface images without crosstalk artifacts and with a higher vertical resolution, it has certain limitations. The precise extraction of different-order multiples is the key to applying imaging methods based on RTM-CM (Liu et al., 2016; Li et al., 2017b). As the backward-propagated virtual primaries in Eq. (9) are generated from the wave-equation modeling using Eqs. (3) and (5), the additional accurate information of the seabed interface is another challenge of the proposed method, especially for real data application. The water layer model can be acquired by the stacking profile of seismic data or the migration result using the water velocity. Compared with the results of primaries and multiples shown by the black arrows in Fig. 12, our approach involves partial illumination loss in the far offset owing to data transformation from the far-offset to near-offset. It is a trade-off between illumination and crosstalk

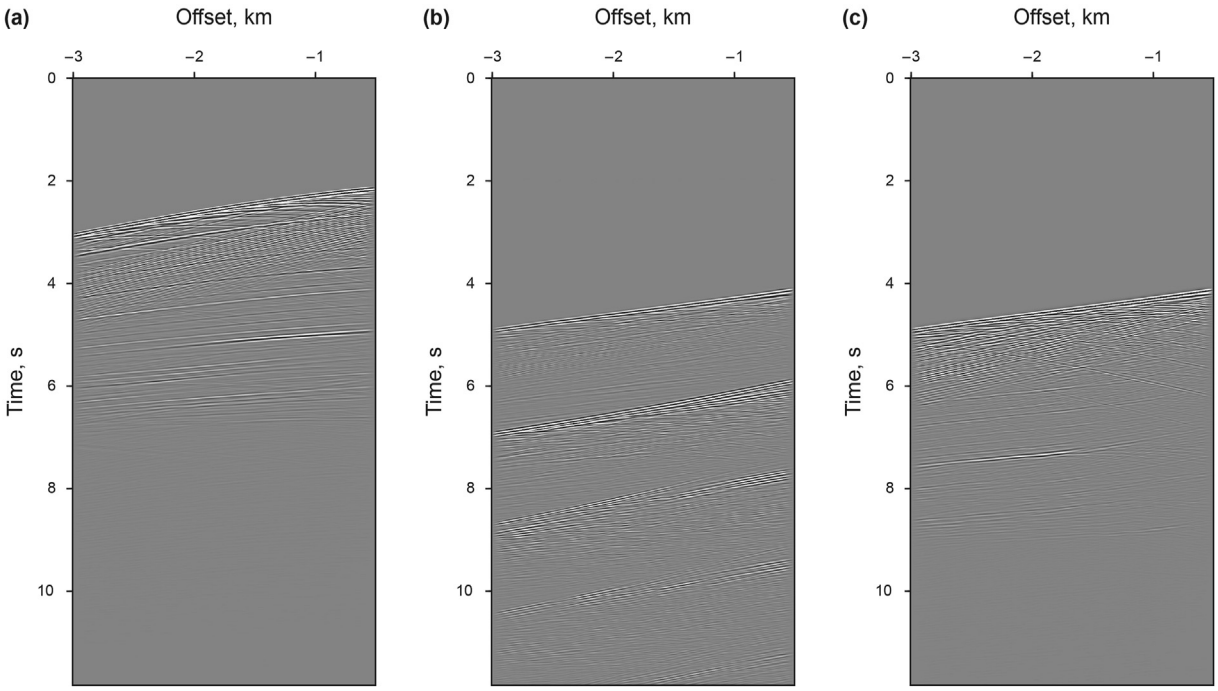

Fig. 11. Seismic records of (a) the primaries, (b) the multiples, and (c) the first-order receiver-side water-bottom-related multiples.

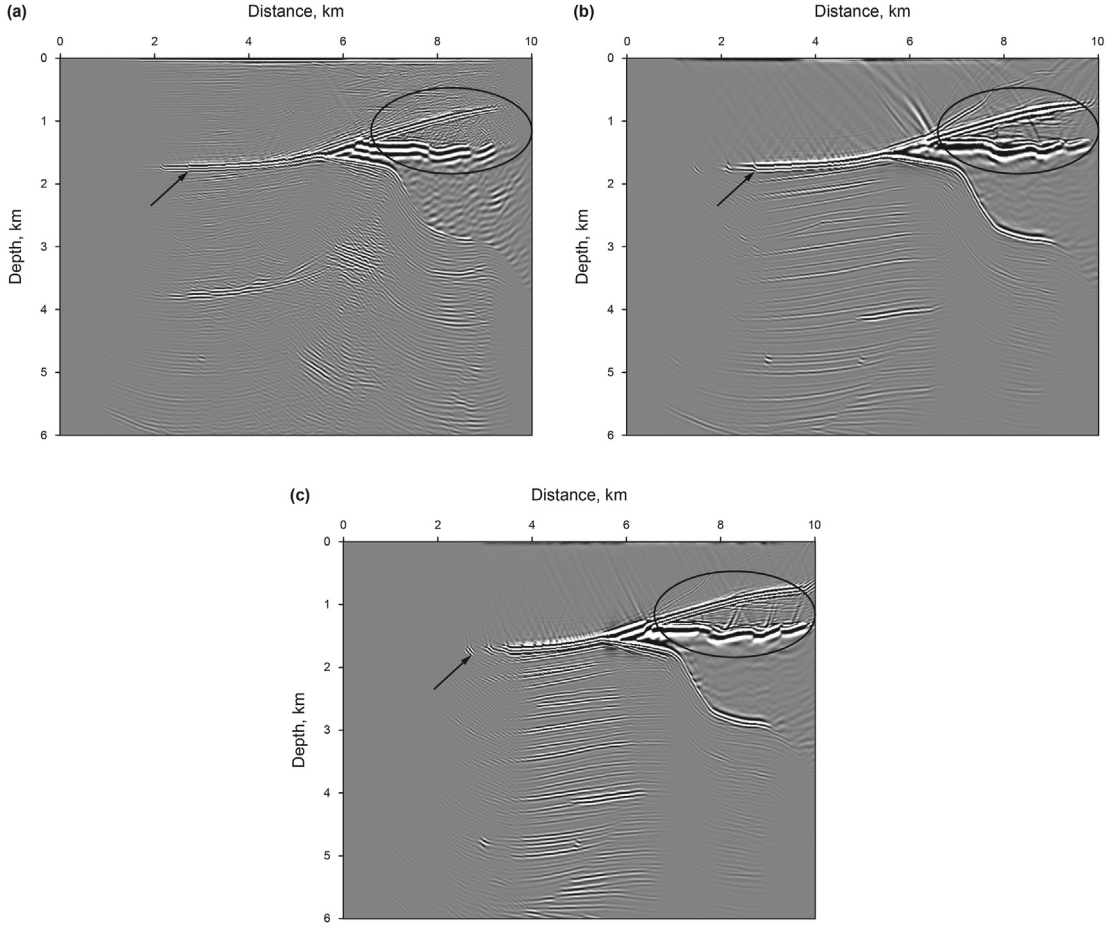

Fig. 12. Migration results of the Sigsbee 2B model. (a) RTM using all orders of multiples, (b) Traditional RTM using primaries, and (c) RTM result by the proposed method. The ellipse in panel (c) shows that the result of our method can depict the reflectors better than both the previous migration methods.

artifacts. To further exploit the smaller reflection angles of multiples information, higher-order receiver-side water-bottom-related multiples can also provide useful information based on Eqs. (3)–(7). Theoretically, the results of the high-order multiple should exhibit higher vertical resolutions than those from the first-order multiples. Therefore, the receiver-side multiples images can be used for AVA (amplitude versus angle) or AVO (amplitude versus offset) analyses for higher vertical resolution, especially for shallow targets. However, the first-order receiver-side multiples of deep strata are difficult to obtain and undergo backward-extrapolation. Therefore, the first-order receiver-side water-bottom-related multiples were employed in this study.

5. Conclusions

In this study, we proposed an imaging strategy utilizing multiples. Unlike the conventional RTM using multiples involving forward- and backward-extrapolation of seismic data, the proposed migration algorithm transforms the first-order receiver-side water-bottom-related multiples into a set of virtual primaries by backward wave equation modeling. The major advantages of this approach include: (1) its production of crosstalk-free images compared with the RTM using multiples and (2), its creation of images with higher vertical resolutions compared with the traditional RTM of primaries. Numerical examples of synthetic velocity models demonstrate that the method developed is an impressive and promising migration algorithm for imaging subsurface structures.

Acknowledgments

The research was partially funded by the National Natural Science Foundation of China (Grant No. 41730425), the Special Fund of the Institute of Geophysics, China Earthquake Administration (Grant No. DQJB20K42), and the Institute of Geology and Geophysics, Chinese Academy of Sciences Project (Grant No. IGGCAS-2019031).

Appendix. Separating multiples into different orders

The main challenge of imaging using multiples is the presence of crosstalk artifacts, and we can classify crosstalks into order-related and event-related crosstalks. Liu et al. (2016) proposed RTM using controlled-order multiples (RTM-CM) to eliminate order-related crosstalks, while Zhang et al. (2020) developed RTM using source-side water-bottom-related multiples to eliminate event-related crosstalks. However, both methods require the prediction of different orders of multiples. To achieve this, we implemented an extended SRME method.

In SRME, the primaries and all-order multiples which are predicted by stacking the time-domain convolution (star *) results of the seismic data can be separated using the following expressions:

$$\begin{cases} R(x_r, x_s, t) = P(x_r, x_s, t) - M(x_r, x_s, t) \\ M(x_r, x_s, t) = \beta(t) R(x_r, x_s, t) * P(x_r, x_s, t) \end{cases} \tag{13}$$

where P denotes the recorded data containing primaries R and all-order multiples $M = \sum_{k=1}^{N} M^k$. $\beta(t)$ represents the adaptive matching filter which can be estimated by minimizing the following equation:

$$f(\beta(t)) = \sum_{x_r} \sum_{t} \{P(x_r, x_s, t) - \beta(t) \widehat{M}(x_r, x_s, t)\}^2 \tag{14}$$

where $\widehat{M} = R*P$ represents the predicted multiples. To produce the isolated-order multiples, for example, the kth-order multiples M^k, we expanded the SRME as follows:

$$\begin{cases} \psi^k(x_r, x_s, t) = \sum_{i=k, k\geq 1}^{N} M^i(x_r, x_s, t) \\ \psi^{k+1}(x_r, x_s, t) = -\beta(t) R(x_r, x_s, t) * \psi^k(x_r, x_s, t) \\ M^k(x_r, x_s, t) = \psi^k(x_r, x_s, t) - \psi^{k+1}(x_r, x_s, t) \end{cases} \tag{15}$$

where ψ^k represents the higher-order multiples with k as the minimum order and N is the maximum order of multiples. For instance, by setting $k = 1$, the first-order multiples M^1 can be extracted by subtracting ψ^2 from ψ^1. To obtain higher-order multiples, the loops in Eq. (15) need to be followed.

References

Bai, L.S., Liu, Y.K., Lu, H.Y., 2020. Interface controlled multiple elimination by sparsity inversion. Commun. Comput. Phys. 28 (1), 459–476. https://doi.org/10.4208/cicp.OA-2018-0077.

Baysal, E., Kosloff, D.D., Sherwood, J.W.C., 1983. Reverse time migration. Geophysics 48 (11), 1514–1524. https://doi.org/10.1190/1.1441434.

Berkhout, A.J., 1982. In: Seismic Migration: Imaging of Acoustic Energy by Wavefield Extrapolation-Ppart a: Theoretical Aspects, second ed. Elsevier.

Berkhout, A.J., Verschuur, D.J., 1997. Estimation of multiple scattering by iterative inversion, Part I: theoretical considerations. Geophysics 62 (5), 1586–1595. https://doi.org/10.1190/1.1444261.

Biersteker, J., 2001. Magic: shell's surface multiple attenuation technique. SEG Tech. Progr. Expand. Abstr. 1301–1304. https://doi.org/10.1190/1.1816335, 2001.

Davydenko, M., Verschuur, D.J., 2017. Full-wavefield migration: using surface and internal multiples in imaging. Geophys. Prospect. 65 (1), 7–21. https://doi.org/10.1111/1365-2478.12360.

Dragoset, B., Verschuur, E., Moore, I., et al., 2010. A perspective on 3D surface-related multiple elimination. Geophysics 75 (5), 61. https://doi.org/10.1190/1.34754 13, 75A245.

Hargreaves, N., 2006. Surface Multiple Attenuation in Shallow Water and the Construction of Primaries from Multiples. SEG Technical Program Expanded Abstracts, pp. 2689–2693. https://doi.org/10.1190/1.2370080.

He, B., Liu, Y.K., Zhang, Y.B., 2019. Improving the least-squares image by using angle information to avoid cycle skipping. Geophysics 84 (6), S581–S598. https://doi.org/10.1190/geo2018-0816.1.

Jin, H., Wang, P., 2012. Model-based water-layer demultiple (MWD) for shallow water: from streamer to OBS. SEG Tech. Progr. Expand. Abstr. 1–5. https://doi.org/10.1190/segam2012-1401.1.

Li, Z.N., Li, Z.C., Wang, P., et al., 2017. Reverse time migration of multiples based on different-order multiple separation. Geophysics 82 (1), S19–S29. https://doi.org/10.1190/geo2015-0710.1.

Liu, X.J., Liu, Y.K., Lu, H.Y., et al., 2017. Prestack correlative least-squares reverse time migration. Geophysics 82 (2), S159–S172. https://doi.org/10.1190/geo2016-0416.1.

Liu, X.J., Liu, Y.K., 2018. Plane-wave domain least-squares reverse time migration with free-surface multiples. Geophysics 83 (6), S477–S487. https://doi.org/10.1190/geo2017-0570.1.

Liu, X.J., Liu, Y.K., Khan, M., 2018b. Fast least-squares reverse time migration of VSP free-surface multiples with dynamic phase-encoding schemes. Geophysics 83 (4), S321–S332. https://doi.org/10.1190/geo2017-0419.1.

Liu, Y.K., Chang, X., Jin, D.G., et al., 2011. Reverse time migration of multiples for subsalt imaging. Geophysics 76 (5), WB209–W216. https://doi.org/10.1190/geo2010-0312.1.

Liu, Y.K., Liu, X.J., Osen, A., et al., 2016. Least-squares reverse time migration using controlled-order multiple reflections. Geophysics 81 (5), S347–S357. https://doi.org/10.1190/geo2015-0479.1.

Liu, Y.K., Liu, X.J., Zhang, Y.B., 2018. Migration of seismic multiple reflections. Chin. J. Geophys. 61 (3), 1025–1037. https://doi.org/10.6038/cjg2018L0368.

Lu, S.P., Whitmore, D.N., Valenciano, A.A., et al., 2015. Separated-wavefield imaging using primary and multiple energy. Lead. Edge 34 (7), 770–778. https://doi.org/10.1190/tle34070770.1.

Luo, S., Hale, D., 2014. Least-squares migration in the presence of velocity errors. Geophysics 79 (4), S153–S161. https://doi.org/10.1190/geo2013-0374.1.

Muijs, R., Robertsson, J.O., Holliger, K., 2007. Prestack depth migration of primary and surface-related multiple reflections: Part I-Imaging. Geophysics 72 (2), S59–S69. https://doi.org/10.1190/1.2422796.

Nemeth, T., Wu, C., Schuster, G.T., 1999. Least-squares migration of incomplete reflection data. Geophysics 64 (1), 208–221. https://doi.org/10.1190/1.1444517.

Rocha, D., Sava, P., 2018. Elastic least-squares reverse time migration using the energy norm. Geophysics 83 (3), S237–S248. https://doi.org/10.1190/geo2017-0465.1.

Shi, Y., Wang, W.H., 2012. Surface-related multiple suppression approach by combining wave equation prediction and hyperbolic Radon transform. Chin. J.

Geophys. 55 (9), 3115–3125. https://doi.org/10.6038/j.issn.0001-5733.2012.09.029.
Verschuur, D.J., Berkhout, A.J., Wapenaar, C.P.A., 1992. Adaptive surface-related multiple elimination. Geophysics 57 (9), 1166–1177. https://doi.org/10.1190/1.1443330.
Wang, P., Jin, H., Xu, S., et al., 2011. Model-based water-layer demultiple. SEG Tech. Progr. Expand. Abstr. 3551–3555. https://doi.org/10.1190/1.3627937.
Yao, G., Wu, D., 2015. Least-squares reverse-time migration for reflectivity imaging. Sci. China Earth Sci. 58 (11), 1982–1992. https://doi.org/10.1007/s11430-015-5143-1.
Yao, G., da Silva, Debens, N.V., et al., 2018. Accurate seabed modeling using finite difference methods. Comput. Geosci. 22 (2), 469–484. https://doi.org/10.1007/s10596-017-9705-5.
Zhang, D.L., Schuster, G.T., 2014. Least-squares reverse time migration of multiples. Geophysics 79 (1), S11–S21. https://doi.org/10.1190/geo2013-0156.1.
Zhang, Y.B., Liu, Y.K., Liu, X.J., 2019. Reverse time migration using controlled-order water-bottom-related multiples. SEG Tech. Progr. Expand. Abstr. 4261–4265. https://doi.org/10.1190/segam2019-3206145.1.
Zhang, Y.B., Liu, Y.K., Liu, X.J., et al., 2020. Reverse time migration using water-bottom-related multiples. Geophys. Prospect. 68 (2), 446–465. https://doi.org/10.1111/1365-2478.12851.
Zhou, X.P., Liu, Y.K., Li, P., 2019. Improved shallow water demultiple method with multichannel prediction operators. Chin. J. Geophys. 62 (2), 667–679. https://doi.org/10.6038/cjg2018M0260.
Zuberi, A., Alkhalifah, T., 2013. Imaging by forward propagating the data: theory and Application. Geophys. Prospect. 61 (s1), 248–267. https://doi.org/10.1111/1365-2478.12006.